International Journal of Applied Engineering Research ISSN 0973-4562 Volume 13, Number 10 (2018) pp. 8490-8506

Effect of High Frequency Power Supplies on the Electrostatic Precipitator Collection Efficiency as Compared to Conventional Transformer Rectifiers

Gerald Chauke and Rupert Gouws
School of Electrical, Electronic and Computer Engineering, North-West University, Potchefstroom, South Africa.

Abstract

Particulate emission is a major problem in industrial processes, caused mainly by power plants that make use of coal as a primary source of energy. Stringent emissions limits, set by government organisations requires industries to conform to these limits to ensure that air quality is sustained and within minimum pollutant limits. Electrostatic precipitators (ESP) are, implemented as the main form of dust burden collection. In recent years, power stations of the national electricity supplier (Eskom) have struggled to maintain particulate emissions below legislation limits, resulting in power stations having to de-load and reduce power generation production. A pilot project was initiated to investigate what the effects of new high frequency power supplies will be on the ESP collection efficiency. This paper presents the results obtained from the implemented pilot project, whereby 16 new high frequency power supplies (HFPS) were installed in a 28 field ESP plant.

Keywords: Electrostatic precipitator, Particulate emissions, High frequency power supplies, Transformer rectifiers.

INTRODUCTION

Electrostatic precipitation (ESP) is a widely used technology for effective dust or fumes collection from industrial furnaces. Dust collection is, achieved by making used of electric forces to collect suspended dust particle in the flu gas streams. This collection process is achieved through the following three step process; 1) first stage of the process involves the charging of the suspended dust particle, 2) second stage of the process is the collection of the charged particles and 3) the final stage involves the removal of the collected/ precipitated material for disposal or other use.

This technology has, been in existence as early as 1906, with break through research conducted by Dr Frederick G. Cottrell and W. A. Schmidt. Dr F. G. Cottrell is an American born professor in chemistry and is, credited as being the inventor of the first electrostatic precipitator [1, 2].

Figure 1 illustrates the position of an ESP plant in a fossil fired power station [3]. Electric forces are, established between a discharge and collector plate arrangement; pathway for the flue gas stream also known as a field. The power station to be investigated for the purpose of this project makes use of a single stage, dry-type, parallel plate arrangement ESP and each unit has four parallel casing each having seven fields in a row, thus has 28 fields per unit.

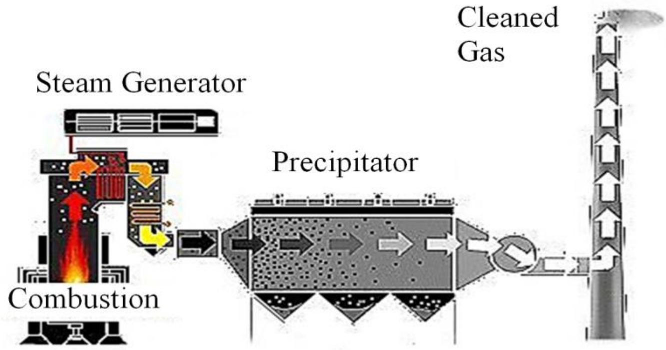

Figure 1: ESP plant as installed in a power station (adapted) [3]

A single stage ESP design is one whose arrangement allows for the charging and collection of dust particles to occur in the same region/field [1, 2]. Each field in an ESP arrangement consists of a discharge wire/active electrode and two collector plates/electrodes on either side of the discharge electrode forming horizontal ducts. Figure 2 illustrates the ESP dust collection, principle operation [4].

Suspended dust particles extracted inside the boiler/ combustion chamber from the boiler by means of an induction fan and enter the ESP fields. The discharge electrodes are, connected to a high voltage negative DC supply in order to produce the corona needed for ionization. There are six fundamental principles involved inside the ESP to achieve dust particulate collection [1, 2]: 1) ionization, 2) migration, 3) collection, 4) charge dissipation, 5) particle dislodging and 6) particle removal.

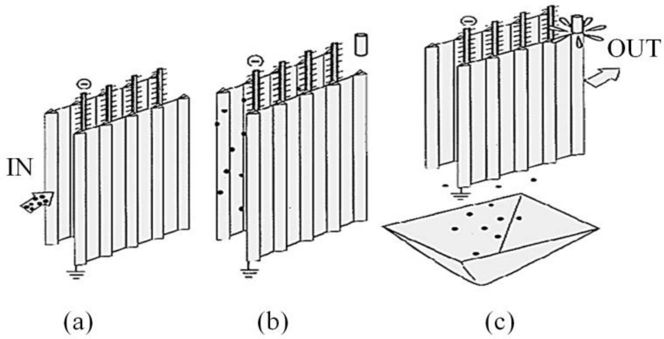

Figure 2: ESP dust collection, principle operation (adapted) [4].

Flue gas enters the ionization region, resulting in dust particles attaining a charge (negative) charge, and through the applied electric field, the charged dust particles migrate to the collector plate and subsequently lose their charge and removed through the rapping process [5].

The ionization process takes place when electrons within the vicinity of the corona discharge are excited/ energized. The electron excitation results in electron collision, which causes an electron avalanche and these electrons, attach themselves to the suspended dust particle passing through the ionized inter-electrode space. The flue gas stream flows through the ionized chamber such that the suspended dust particles acquire a charge, thus particle separation. The particles attain a negative charge and deflecting them out of the flue gas stream, due to the presence of the electric field established by the presence of high voltage DC. The charged particles deflect and migrate to the positively charged collector plate under the influence of the electric field for collection. The collected dust burden is, retained on the collector plate and subsequently dislodged periodically by a rapping process. The rapping process makes use of a hammering system that strikes the collector plate, dislodging the dust burden into ash hopers to collected and transported to the ash dump. This process removes more than 98% of solid dust particles [1, 2, 4, 6, 7].

Particulate emissions in South African context

Particulate emissions are governed by the air quality legislation, which requires the operation of a power station to comply with the stipulated emissions limits at all times during operation. Failure to comply with stipulated emissions limits as specified by the legislation carries a stiff fine or even jail time. In order to comply with the set out emissions limits, power stations have resorted to taking load losses; reduction in boiler production capacity in order to reduce particulate emissions. The practice of taking load losses due to ineffective ESP performance is a costly exercise, as the power stations lose revenue for every MW that is not generated. This also puts further constraints on the power grid; the inability to produce power has negative implications for the country. South Africa has had a power shortage crisis since 2007, which resulted in load shedding being implemented. The reduction in production load as a result of high stack emissions, further increases the pressure on an already constraint power grid, and contributes to load shedding.

ESP ELECTRICAL SUPPLY

The existing power supply system for the ESP's within the Eskom environment are what are termed conventional rectifier transformer sets. Rectifier transformers make use of 50 Hz mains frequency and are thyristor controlled to deliver the required corona power into the ESP fields. Due to the deterioration in plant and process conditions, the rectifier transformers have proven ineffective, as they are unable to supply and maintain the required corona power to effectively collect the dust particulates and ensure compliance to particulate emissions regulations. The authors of [17] provide the electrical circuitry representation of a convention rectifier transformer, connection to an ESP field.

The transformer set, delivers a high DC voltage that is, coupled with an AC ripple. The generated ripple has a 50 Hz mains frequency and the amplitude (peak-to-peak) of this ripple has been, found to be in the range of 30 to 40% of the output DC voltage [8]. This significantly reduces the average DC output voltage and limits ESP performance. The operating ESP voltage is primarily limited by sparking, and a spark typically occurs on the peak of the AC ripple voltage [1, 2]. The control system is design in such a way that, when a spark is, detected the control reduces a certain percentage of the voltage.

A high percentage, ripple voltage effect, results in significant voltage reduction when sparking occurs and subsequent reduction in corona power. The reduced average voltage, results in the reduction in the effective electric field intensity that is required to repel the charged particulates for collection. This results in ineffective charging and collection of the dust particulate. The delivered corona power needs to be, optimized in order to improve the ESP collection efficiency.

ESP collection efficiency is, influenced by the generated electric field as stipulated by the Deutch's efficiency formula [1, 2]. Thus, increasing the corona power; voltage and current, input into the ESP fields improves the collection efficiency of the field.

Power supply influence on ESP efficiency

Deutch's [1, 2] efficiency formula is primarily used in determining ESP collection efficiency, the efficiency is defined as a function of the migration velocity (ω), effective collection area (A) and the volumetric gas flow (Q):

$$\eta = 1 - e^{\left(-\omega \cdot \left(A/Q\right)\right)} \quad (1)$$

Where Q is the volumetric gas flow, A is the total projected collecting electrode area, and ω is the effective particle migration velocity.

The effective collection area of the ESP is fixed and is given by collector plate area, thus a redesign would be required, if it were to be used to influence the efficiency. An increased volumetric flow will reduce the overall efficiency; hence, the particle migration velocity is one aspect that can be, evaluated to optimise the collection efficiency. The migration velocity is, defined as is dependent on the displacement electric field and is, defined as:

$$\omega = K.E_0.E_C.a^2 \quad (2)$$

Whereby, E_0 is the charging electric field and E_C is the collection electric field, K is a constant and a, is the particle radius. Eskom makes use of single stage ESP's and for these ESPs, the charging and collection occurs simultaneously, thus;

$$E_0 = E_C \quad (3)$$

Hence, the particle migration velocity can be, expressed as:

$$\omega = K.E^2.a^2 \quad (4)$$

The relationship between the electric field and the migration velocity highlights the fact that, the removal and retention of dust burden is directly dependent on the corona ionisation and the electric field strength. The velocity of a charged particle moving through an electric field is proportional to the applied voltage. Thus, high levels of electrical energization need to be, maintained in order improve the collection efficiency of the system.

White [8] also states that the migration velocity can be, defined as a function of the corona current and the kV input with the superimposed ripple voltage. Thus, further highlighting the importance of the voltage ripple effect on the collection efficiency:

$$\omega = (I_{DC}).(kV_{peak}).(kV_{DC}) \quad (5)$$

Increasing the particle migration velocity can only be, achieved by increasing the electric field and this is, achieved by increasing the kV input into the ESP fields. The particle size is a quantity that is process dependant and cannot be, varied at will. Therefore, the migration velocity of a charged particle moving through an electric field will be proportional to the square of the applied voltage.

The operating ESP voltage level is, limited by the occurrence of flashovers, and as such, the voltage is required to be high enough that some sparking occurs. Sparking results in loss of power, thus reducing the corona input required for ionization.

The operating DC voltage is typically limited by the sparking that occurs during operation, sparking occurs at the peak of the voltage ripple. However, the collection efficiency is at its highest when the voltage is closest to the spark inception voltage, i.e. peak voltage of the ripple. Sparking results in loss of power and as a result, less power is used for the corona. Reducing the ripple to be near the spark over voltage will increase the effective DC input voltage. Increasing the DC input voltage results in an increased intensity of the effective collection electric field present in the inter-electrode spacing. The electric field repels the charged particles and the strength of the electric field will influence the particle migration velocity. Migration velocity is the velocity at which the charged particle is drawn toward the collector plate; a high migration velocity is desired to effective particle collection.

The ripple effects, plays a vital role in increased kV input into the ESP fields and high Frequency switching appears to provide the capability to increase the kV supply the ESP fields. The voltage ripple is inversely proportional to the switching frequency and the load capacitance. The corona current does not vary significantly in ESP operation and is a function of the change in charge with time.

$$i = \frac{dq}{dt} \quad (6)$$

Charge can be, expressed as a function of capacitance and potential difference; the potential difference refers to the voltage ripple's peak-to-peak quantities as they represent the time constant for voltage decay within the capacitor.

$$q = C\Delta V \quad (7)$$

Substituting the charge function into current gives the following expression for voltage ripple:

$$i = \frac{dq}{dt} = C\frac{dV}{dt} = C\frac{\Delta V}{\Delta t} \quad (8)$$

$$\Delta V = \frac{\Delta t.i}{C} \quad (9)$$

Δt is the conduction/switching time of a semiconductor and this determines the voltage ripple frequency.

$$\Delta t = \frac{1}{f} \quad (10)$$

Hence:

$$\Delta V = \frac{i}{f.C} \quad (11)$$

ESP's operating with convention 50 Hz transformers will obviously have a higher voltage ripple as compared to transformer sets operating at high frequency range. As previously stated, the quantity of the ripple influences the overall average DC output voltage, which is dependent on the resonance capacitance. The influence of the produce ripple can be, expressed as follows:

$$V_{avg} = \sqrt{(V_{DC})^2 \pm (V_{DC} \times \%V_{ripple})^2} \quad (12)$$

Thus, the ripple affects the ionization and collection process as a whole.

The Corona power is, significantly increased by effectively reducing the voltage ripple and increasing the ESP input DC voltage. White defines the corona power as a product of the input voltage and the corona current flow.

$$W = (I_{DC}).(KV_{DC}) \quad (13)$$

$$W = (I_{DC}).\left(\frac{KV_{max-peak} + KV_{min-peak}}{2}\right) \quad (14)$$

KV_{DC} is the average DC system voltage input.

A higher, average power supply into the, ESP fields, the stronger and more intense electrostatic field. This means that the time needed to treat a particle can be much shorter compared to conventional transformers. This in return results in more effective particle charging. The higher the electrical field strength the faster is the migration velocity (the velocity at which the charged particle is drawn towards the collector electrode). The ESP efficiency is, calculated using the Deutsch formula and it is a function of the migration velocity as indicated in equation (1) [1, 2, 9-15, 17, 18].

HFPS PILOT PROJECT SCOPE

The pilot test project required the retrofitting of 16 new HFPS transformers on a 28 field ESP, with four casings. Each casing consists of 7 fields, and the first four front fields are to be retrofitted with new HFPS transformers. Figure 3, illustrates the ESP plant power supply transformers configuration.

Figure 3: ESP power supply arrangement.

The scope required to be executed in order to retrofit the new HFPS transformers involved electrical, mechanical and control & instrumentation work. Work was conducted during an outage, while the unit was shut-down for maintenance. Maintenance work was also conducted on the internals of the ESP, in order to restore its internal mechanical condition.

Electrical modification

Two substations supply power to ESP transformers, each substation supplying the LH or RH casing respectively. Inside the substation, the 380 V supply from the 380 V precipitator board is connected to the precipitator control cabinets (also referred to as the High Tension panel or HT panel) of each transformer; 14 control panels per substation. From the HT panels, cables are, routed to the precipitator roof, where the precipitator transformer-rectifiers are located.

The electrical system was, configured to supply single phase 380 Vac, as the conventional TR require single-phase power. The installation of the new HFPS requires a 3-phase supply and thus the plant had to be modified such that it supplies 3 phase. Work carried out required the modification of the supply boards, installing new cabling from the bus-section to the control cubicle and all the way to the precipitator roof.

The installation and commissioning of the HFPS transformers was, conducted while the unit was online. The online installation and commissioning was, done on a casing-by-casing basis; the first four TR sets were isolated and decommissioned. Installation started on the fourth field, moving upstream; from fourth field to the first field. The reason for implementing this installation methodology was for safety reasons. The upstream fields have to be isolated, in order to avoiding charge carry-over that can discharge of fields worked on and possibly create an unsafe working environment. Upon completion of the HFPS transformers, a settling and proving period was, observed for a period of about 2 to 3 months weeks, while monitoring the performance of the ESP. Figure 4 shows the new HFPS transformer installation.

Figure 4: New HFPS transformer installation.

Control and Instrumentation modification

The signals from the new HFPS controllers had to be, interfaced with the existing precipitator plant management system (PPMS). The PPMS consists of a PLC (Sixnet) as an automatic control system and a SCADA (Citect) using communications interfaces of Modbus (CANbus) and Ethernet. The rapping on all seven fields is, managed and controlled by the existing PPMS. The electrical parameters on the newly installed are HFPS on the first four fields are controlled by the new HFPS controllers and the last three fields will still be controlled by the existing PPMS. The new HFPSs controllers are, interfaced to the SCADA via the existing PLC. The PLC was, expanded/programmed to accommodate the new HFPS controllers. Figure 5 illustrates the configuration of the control and instrumentation integrated into the existing control and monitoring system.

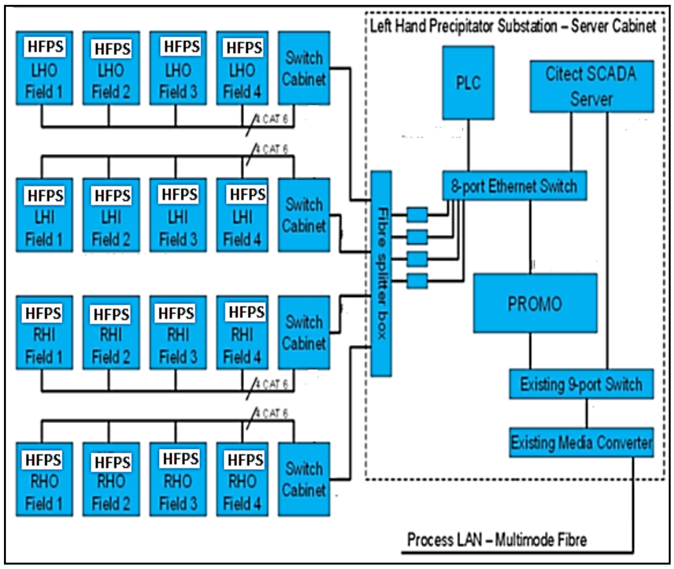

Figure 5: New HFPS control system configuration.

The control system of the new HFPS provides the following information to the PPMS, for monitoring purposes: Primary current, Primary Voltage, Secondary Current, Secondary Voltage, Sparking and Arc rate, Power output, and Fault indication.

The control thereof of the new HFPS is, achieved by the use of the ProMo system; this is to optimize the new HFPS by changing settings, as and when required. The ProMo system was, integrated into the PPMS, as it can only control the new HFPS transformer, whereas the fifth, sixth and seventh fields still made use of the PPMS. This system has the capability to plot V-I curves, in order to analyse the status and conditions of the fields with the new HFPS. Similarly, to the PPPMS, different modes of operations can be selected; continuous or pulsing mode, depending on the operating conditions. Pulsing mode, is typical implemented whenever, the ESP is receiving high resistivity ash in instances when the SO3 plant is not available to condition the flue gas. For the purpose of this projected, the pulsing mode operation and effectiveness thereof was, not evaluated.

Rapping Philosophy

The rapping philosophy implemented in the station, is a queuing rapping philosophy. Queuing refers to the sequence in which rapping is triggered for the fields, this philosophy is to ensure that two fields in the same casing never rap during the same time interval and thus reduces emissions rapping spikes. The front fields (Fields 1, 2 and 3) collected most of the flue gas, and thus have to be, rapped more frequently as compared to the rear fields. The queuing process, gives priority to the front fields, meaning if ever there is a scenario where the sixth field is, triggered to start rapping at the same time as field 2, field 7's rapping will be, delayed and thus allowing field 2 to rap firsts and field 7 will only rap once field 2 has completed its rapping. This rapping process is, controlled by the PPMS, based on the timer setting input on the AVC for each field.

The PPMS has several programmes loaded on it and these programmes control the performance of the ESP fields, particularly for rapping. Programmes 1, utilized during normal operation on the unit and each program has specific rapper timer settings; intervals and duration. The implemented operating programmes utilized are as follows:

Table 1: Rapping philosophy for TR set.

Field	Interval (Minutes)	Duration (Seconds)	Vs Lim	Rap enabled
1	10	35	0	Rap 1
2	18	35	0	Rap 1
3	30	35	0	Rap 1
4	55	35	0	Rap 1
5	95	35	0	Rap 1
6	170	35	0	Rap 1
7	1440	1	0	Rap 1

The new HFPSs were, installed, and commissioned over a period of 5 weeks, the installation and commissioning was, conducted per casing. Optimisation, of the ESP was, conducted for a period of a week; optimisation involved changing the rapping regime, from that which was, implemented for the conventional power supply system. It was, expected that the four field with the newly installed HFPS technology would collect more dust burden and thus, the rapping frequency was increased.

The rapping frequency of the last three fields was, also changed according; since the front four fields will collect the most dust burden, the rapping frequency of the rear fields was reduced. An additional rapping feature that was, implemented was the power down rapping (PDR). This form of rapping occurs with the field de-energised and occurs after a set cycle of normal field rapping. The controller sends a signal, to the new HFPS to switch of allowing the rapping to occur, the intention for implementing this rapping philosophy was to ensure that the collected plates are, kept clean for improved collection efficiency. Table 2, illustrates the new rapping settings implemented for the installation of the new HFPS.

Table 2: Rapping philosophy implemented for the new HFPS.

Field	Normal rapping		PDR	
	Interval	**Duration**	**Interval**	**Duration**
1	6 min	35 sec	30 min	35 sec
2	10 min	35 sec	1 h	35 sec
3	30 min	35 sec	3 h	35 sec
4	3 h	35 sec	12 h	35 sec
5	8 h	35 sec	24 h	35 sec
6	24 h	35 sec	48 h	35 sec
7	48 h	35 sec	48 h	35 sec

ESP EFFICIENCY TESTING

ESP efficiency tests were, conducted by an external party, for both conventional TR set and HFPS power supplies. An ESP efficiency test, is a Gravimetric test (EPA Method 17) [6, 16], that measure the volume dust burden entering the ESP and that exiting the ESP. The percentage difference of the outlet as compared to the inlet is an indication of the collection efficiency of the ESP system.

A baseline line, ESP efficiency test was, conducted with conventional TR set power supply. A post HFPS installation, ESP efficiency test was, also conducted, to determine performance of the ESP. These tests, were conducted under identical loading conditions, however they were conducted approximately 4 months apart and the resulted obtained results were correlated by making use of Eskom approved correction curves. The following procedure was conducting the efficiency tests:

Required Operating Conditions

All the tests were, carried out at 618 MW unit loads, with the plant having operated steady at this load for a period of 24-hours and during the testing period. The following plant parameters were, recorded and monitored during the testing period: 1) ESP fields in service, 2) Electrical condition of fields (Obtained from PPMS), 3) Secondary voltage and current, and 4) Process conditions; inlet and outlet temperatures.

Isokinetic dust sampling

Five isokinetic tests were, carried out at each duct; with each inlet duct being equipped with four sampling ports and the outlet duct having six sampling ports. Four sets of sampling equipment were used simultaneously and placed so that two casings are, traversed sequentially by one set of equipment [16]. An effort was, made to start and stop the isokinetic sampling simultaneously on all casings, more especially the corresponding inlet and outlet positions on a specific ESP Casing. A probe was, inserted to the deepest point in the traverse where sampling started.

The traversing started simultaneously on the RH Outer and LH Inner and progressed to the RH Inner and LH Outer. The obtained data was, captured for each ducting, analysed and averaged out to determine the combine collection efficiency of the ESP. These results will be the bases of determining and quantifying the exact reduction or lack thereof, in the ESP as, a result of implementing two types of power supply technologies.

ESP EFFICIENCY TEST RESULTS

The ESP performance test was, conducted for both power supply technologies; the test mainly focuses on the process parameters, in terms of flue gas volume flow in and out of the ESP and other process conditions such as coal quality. Isometric sampling was, conducted on the inlet and outlet duct of the ESP casings, these representative samples are, used to determine the collection efficiency of the ESP. Particulate emission measurements were, carried out employing procedures and equipment that comply with the requirements of EN 13284-1 [17], [19]. The VDI correlation procedure was, followed in the determination of the linear regression of the correlation spot check. The baseline ESP efficiency test was, conducted with conventional TR sets installed and thereafter, a second efficiency test was, conducted with the new HFPS installed.

Baseline ESP efficiency test with TR set

Five ESP efficiency tests were, conducted on the unit, while operating at full load of 618 MW generated load. Table 3, illustrates the obtained results from the isometric testing conducted during the ESP efficiency test. The average efficiency of the ESP post outage and with conventional TR sets was, found to be 97.1%; emitting at 42.8 mg/Nm^3, at an average boiler load of 619 MW.

Table 3: Isometric ESP efficiency test results.

Test no.	Boiler Load	% of Total Air flow	Standard Deviation (% of Total air flow)	Effective emissions	Dust Concentration	Average isokineticity	average O2 Concemtration at ESP inlet
	MW	kg/s	%	-	mg/Nm^3 at 10% O2	%	mm
1	618.8	580.6	1.4	73.7	30.3	97.8	4.8
2	619.2	572.7	1.2	34.3	18.1	98.2	4.3
3	618.9	581.4	1.1	40.5	19.2	95.9	4.4
4	619.1	573.6	1.0	32.0	22.9	96.7	4.5
5	619.2	575.1	1.1	33.7	15.4	96.8	4.6
Average	619.0	576.7	1.2	42.8	21.2	97.1	4.5

Post HFPS installation ESP efficiency test

The ESP efficiency test was, subsequently performed after the optimisation process had, been completed. Table 4, gives the obtained results for the efficiency test conducted with the new HFPS installed, on the first four fields of the ESP casings. The emissions were, found to be 19.3 mg/Nm^3 and were, maintained at this level consistently.

Table 4: ESP efficiency test results post HFPS installation.

Test no.	Boiler Load	% of Total Air flow	Standard Deviation (% of Total air flow)	Effective emissions	Dust Concentration	Average isokineticity	average O2 Concemtration at ESP inlet
	MW	kg/s	%	-	mg/Nm^3 at 10% O2	%	mm
1	618.2	594.7	1.1	19.3	36.5	95.0	7.1
2	619.5	598.2	1.1	20.3	28.9	96.1	6.8
3	618.6	599.0	1.0	24.0	34.4	95.4	6.8
4	619.6	579.4	1.1	13.8	7.3	98.1	6.2
5	619.7	587.9	0.6	19.1	17.7	98.4	7.1
Average	619.1	591.8	1.0	19.3	25.0	96.6	6.8

It can, be, seen from table 4, that the ESP was experiencing higher flue gas volume flows, as compared to those measured on the baseline efficiency test. For the post, HFPS installation efficiency test the volume flow have increased by up to 21% on some casings and the dust concentration have increased by up to 22% on some of the casings. However, despite these increases in the process conditions, the obtained emissions were less that those obtained in the baseline tests, giving a 45% emissions reduction from baseline.

Electrical performance for both technologies

A field by field electrical performance was conducted for the front four fields. The electrical performance was taken post outage for the conventional TR sets and subsequently post optimization of the new HFPS. The voltage and current measurements were taken for an hour's operation during the ESP efficiency test.

The electrical performance comparison was, conducted for each of the first four fields; for the operation of a conventional TR set and that of a HFPS transformer. The analysis focuses on the power input delivered into the field, as well as the ripple effect contained in voltage delivered into the fields. The presented electrical waveforms were taken from the plant historian, which records the measured plant operating parameters in accordance to the Metering and Measurement Systems for Power Stations in Generation Standard; 240-563590.

The graphs shown data collected during the ESP efficiency test for each power supply technology. The data is sampled at every 30 seconds and averaged out to give an hourly average, which was used to plot the electrical performance. The unit was at a fixed load of 618 MW, for both instance when data was captured.

Table 5, illustrates the collected electrical data during the process of conducting the ESP efficiency tests. The data was taken for a period of 24 hours; from midnight to midnight. The data was put in the same table although the two overall ESP efficiency tests were conducted 3 months apart.

Table 5: LHO 1 current and voltage measurement during the ESP efficiency tests for TR set and the new HFPS.

	LHO 1			
Time	TR Set - LHO 1 Is	TR Set LHO 1 Vs	HFPS- LHO 1 Is	HFPS- LHO 1 Vs
00:00 - 01:00	283.55	26.45	929.68	39.72
01:00 - 02:00	102.28	39.67	1291.92	46.97
02:00 - 03:00	81.02	40.22	1288.32	48.08
03:00 - 04:00	96.50	41.38	1227.78	47.58
04:00 - 05:00	97.93	41.58	890.95	45.81
05:00 - 06:00	96.22	41.47	892.33	45.83
06:00 - 07:00	115.07	41.88	455.28	31.50
07:00 - 08:00	92.77	40.83	15.35	14.41
08:00 - 09:00	104.63	42.03	949.97	43.20
09:00 - 10:00	99.12	40.95	983.25	45.76
10:00 - 11:00	75.90	38.33	858.48	44.93
11:00 - 12:00	69.65	38.52	927.92	45.47
12:00 - 13:00	76.40	38.82	1031.70	48.61
13:00 - 14:00	88.87	39.77	1068.35	46.43
14:00 - 15:00	70.93	38.60	1052.17	48.52
15:00 - 16:00	79.45	39.60	790.88	43.79
16:00 - 17:00	98.78	41.70	850.22	45.05
17:00 - 18:00	95.22	40.55	631.03	39.76
18:00 - 19:00	100.98	39.27	15.83	13.45
19:00 - 20:00	89.10	40.25	20.88	16.17
20:00 - 21:00	116.57	41.03	16.87	15.26
21:00 - 22:00	105.47	41.52	23.65	15.99
22:00 - 23:00	115.93	42.52	21.57	17.30
23:00 - 00:00	137.52	43.28	24.77	17.02

Figure 6 illustrates the difference in electrical performance of the LHO 1 field, when supplied by a TR set and when supplied by an HFPS.

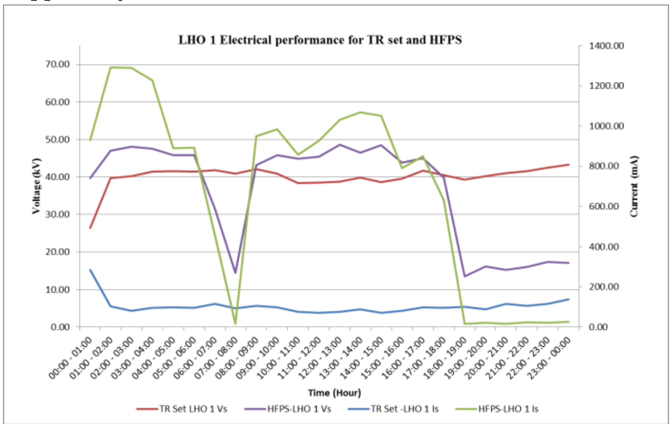

Figure 6: LHO 1 electrical performance for TR set and HFPS.

It can be seen from figure 6, that the electrical performance of LHO 1 field increased significantly. The current input into the field went from below 300 mA for a TR set and could be maintained above 600 mA twice that which the TR set was able to supply. The voltage also increase from low 40 kV for a TR set, to above 40 kV, with the highest voltage being 48 kV supplied by a HFPS. This was a drastic improvement seen on the first field, with consideration that no mechanical repairs were conducted internal from when both measurements were conducted. Table 6 illustrates the collected electrical data during the process of conducting the ESP efficiency tests.

Table 6: LHO 2 current and voltage measurement during the ESP efficiency tests for TR set and the new HFPS.

	LHO 2			
Time	TR Set LHO 2 Is	TR Set LHO 2 Vs	HFPS- LHO 2 Is	HFPS- LHO 2 Vs
00:00 - 01:00	625.03	33.88	1585.60	40.92
01:00 - 02:00	963.75	46.65	1672.37	42.75
02:00 - 03:00	955.55	47.38	1667.87	42.67
03:00 - 04:00	976.98	47.52	1642.47	42.30
04:00 - 05:00	1004.50	47.12	1625.73	43.64
05:00 - 06:00	919.13	47.65	1625.73	43.64
06:00 - 07:00	819.90	46.50	1539.40	46.21
07:00 - 08:00	914.23	47.20	1403.23	48.06
08:00 - 09:00	957.87	48.08	1675.82	44.82
09:00 - 10:00	931.30	47.53	1636.65	43.10
10:00 - 11:00	792.73	46.93	1665.83	44.49
11:00 - 12:00	731.53	45.98	1629.48	43.83
12:00 - 13:00	693.35	46.35	1642.83	43.79
13:00 - 14:00	737.95	46.20	1644.15	43.35
14:00 - 15:00	665.92	46.82	1640.50	42.90
15:00 - 16:00	678.77	46.40	1647.78	45.60
16:00 - 17:00	614.22	44.98	1636.32	45.78
17:00 - 18:00	580.15	45.43	1471.87	46.14
18:00 - 19:00	626.52	45.37	794.10	46.20
19:00 - 20:00	583.88	45.55	920.70	45.45
20:00 - 21:00	753.08	45.50	1035.22	46.78
21:00 - 22:00	748.55	46.10	1301.20	48.61
22:00 - 23:00	755.73	46.10	1113.18	47.42
23:00 - 00:00	800.33	47.18	1071.32	47.39

The current and voltage measurement as presented in table 6 are for both power supply technologies. The data was used to plot the electrical performance of the LHO 2 field; as seen on figure 7.

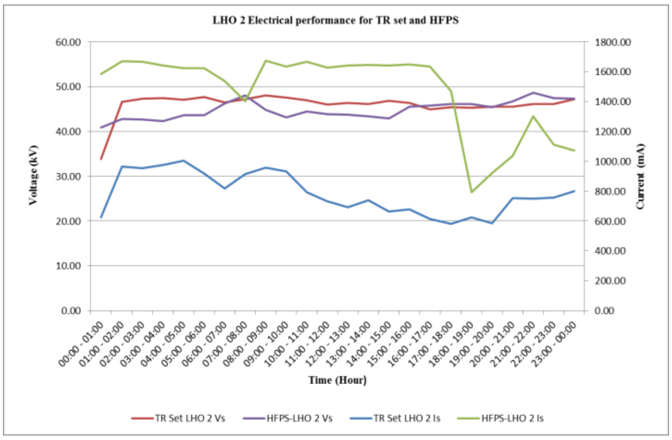

Figure 7: LHO 2 electrical performance for TR set and HFPS.

The electrical performance of the LHO 2 field saw an improvement in the current and voltage, when the HFPS was installed in place of TR set. The TR set was able to supply and maintain a current of about 900 mA, however with the HFPS was able to produce current above 1600 mA. The voltage input into the field did not change drastically, although the TR set was producing a little more voltage as compared to the HFPS.

Table 7: LHO 3 current and voltage measurement during the ESP efficiency tests for TR set and the new HFPS.

	LHO 3			
Time	TR Set LHO 3 Is	TR Set LHO 3 Vs	HFPS-LHO 3 Is	HFPS-LHO 3 Vs
00:00 - 01:00	1110.50	20.87	1555.85	47.18
01:00 - 02:00	1659.88	31.82	1698.92	48.46
02:00 - 03:00	1654.35	31.90	1690.50	47.66
03:00 - 04:00	1655.33	31.82	1671.05	46.35
04:00 - 05:00	1645.63	31.70	1678.07	46.67
05:00 - 06:00	1667.40	31.93	1678.08	46.67
06:00 - 07:00	1661.70	32.45	1650.28	46.38
07:00 - 08:00	1691.63	32.17	1623.05	47.54
08:00 - 09:00	1625.50	31.60	1642.88	46.26
09:00 - 10:00	1702.77	32.02	1699.52	46.81
10:00 - 11:00	1656.98	31.85	1686.88	46.41
11:00 - 12:00	1674.73	31.93	1646.13	45.92
12:00 - 13:00	1645.87	31.83	1670.73	46.34
13:00 - 14:00	1646.75	31.77	1655.83	46.01
14:00 - 15:00	1651.70	31.98	1670.95	45.89
15:00 - 16:00	1532.15	31.85	1697.13	46.92
16:00 - 17:00	1452.08	31.90	1685.03	47.18
17:00 - 18:00	1283.38	32.15	1639.25	46.34
18:00 - 19:00	1432.37	33.08	1558.42	49.48
19:00 - 20:00	1322.60	32.90	1427.40	49.50
20:00 - 21:00	1418.30	32.93	1323.13	49.54
21:00 - 22:00	1590.50	32.52	1556.83	49.77
22:00 - 23:00	1535.72	32.35	1521.00	49.51
23:00 - 00:00	1544.75	32.57	1568.50	50.87

Table 7 illustrates the collected electrical data during the process of conducting the ESP efficiency tests.

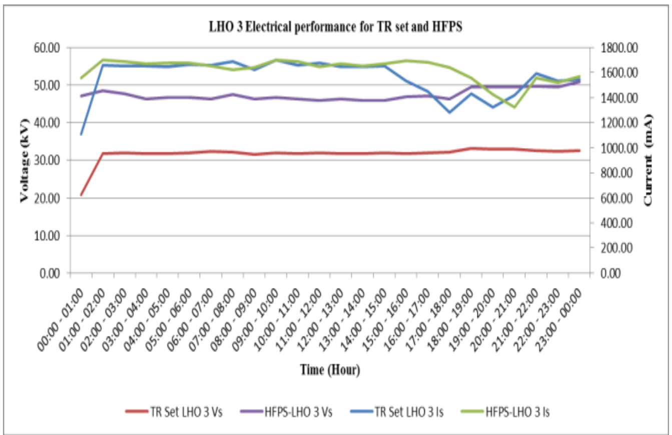

Figure 8: LHO 3 electrical performance for TR set and HFPS.

Figure 8 represent a graphical plot of the LHO 3 electrical performance for both TR set and HFP. The only significant difference that was noted from the two supply technologies was that the HFPS was able to input a high voltage into the field than that of the TR set. The HFPS was able to maintain a voltage of above 47 kV, whereas the TR set could only maintain voltage a low 30 kV. The current input into the field for both transformers was at maximum. The higher voltage, from the HFPS increases the electric field strength for the capturing of the charged dust particles.

Table 8: LHO 4 current and voltage measurement during the ESP efficiency tests for TR set and the new HFPS.

	LHO 4			
Time	TR Set LHO 4 Is	TR Set LHO 4 Vs	HFPS-LHO 4 Is	HFPS-LHO 4 Vs
00:00 - 01:00	413.12	31.37	1179.27	47.31
01:00 - 02:00	471.22	47.52	1472.15	52.89
02:00 - 03:00	455.52	46.87	1535.22	52.52
03:00 - 04:00	458.73	47.35	1636.83	53.28
04:00 - 05:00	460.37	46.98	1668.25	53.11
05:00 - 06:00	462.22	47.28	1668.25	53.10
06:00 - 07:00	482.37	48.40	1679.45	53.45
07:00 - 08:00	483.78	48.08	1649.52	52.74
08:00 - 09:00	474.43	47.80	1655.88	53.52
09:00 - 10:00	487.07	48.23	1642.02	52.08
10:00 - 11:00	485.35	48.93	1671.10	52.87
11:00 - 12:00	434.08	46.23	1671.10	52.92
12:00 - 13:00	409.07	46.48	1683.03	53.77
13:00 - 14:00	405.20	46.67	1645.32	52.76
14:00 - 15:00	357.73	45.47	1668.93	53.08
15:00 - 16:00	385.72	46.00	1655.90	52.53
16:00 - 17:00	389.45	46.53	1627.23	51.88
17:00 - 18:00	393.50	46.55	1673.17	53.14
18:00 - 19:00	413.08	47.32	1536.95	50.89
19:00 - 20:00	416.63	46.80	1470.83	51.26
20:00 - 21:00	422.10	47.05	1361.72	50.89
21:00 - 22:00	407.08	46.45	1567.82	52.60
22:00 - 23:00	440.37	48.15	1543.58	52.20
23:00 - 00:00	392.26	47.36	1571.73	52.65

Table 8 illustrates the collected electrical data for LHO 4 during the process of conducting the ESP efficiency tests. The LHO 4's electrical performance is, illustrated on figure 9; as per data presented on table 8.

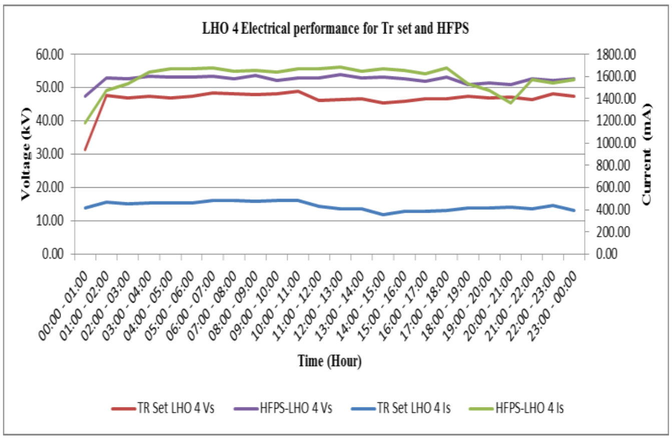

Figure 9: LHO 4 electrical performance for TR set and HFPS.

The LHO 4's electrical performance improved significantly with the installation of the HFPS. The current input into the ESP field increased from around 400 mA to full rated input current of 1600 mA. The voltage input into the field also increase from around 48 kV to 53 kV.

Table 9: LHI 1 current and voltage measurement during the ESP efficiency tests for TR set and the new HFPS.

	LHI 1			
	TR Set LHI 1 Is	TR Set LHI 1 Vs	HFPS-LHI 1 Is	HFPS-LHI 1 Vs
00:00 - 01:00	112.57	37.87	1521.53	42.07
01:00 - 02:00	188.88	55.18	1588.55	44.27
02:00 - 03:00	203.73	53.87	1576.48	44.45
03:00 - 04:00	195.95	53.93	1462.47	43.77
04:00 - 05:00	192.93	53.77	588.53	42.13
05:00 - 06:00	189.20	55.05	577.75	42.09
06:00 - 07:00	198.18	54.17	366.45	39.20
07:00 - 08:00	210.83	55.72	305.73	38.34
08:00 - 09:00	236.52	54.90	747.92	41.24
09:00 - 10:00	241.58	54.97	682.05	41.29
10:00 - 11:00	247.75	53.52	845.25	42.81
11:00 - 12:00	245.62	52.65	628.42	42.47
12:00 - 13:00	252.37	52.37	754.42	40.98
13:00 - 14:00	216.43	54.35	1225.30	44.70
14:00 - 15:00	249.57	52.23	1093.48	42.69
15:00 - 16:00	221.98	52.10	654.68	40.94
16:00 - 17:00	30.87	2.03	611.18	41.21
17:00 - 18:00	0.00	0.00	419.38	39.77
18:00 - 19:00	0.00	0.00	209.07	36.94
19:00 - 20:00	0.00	0.00	208.63	37.29
20:00 - 21:00	0.00	0.00	238.30	37.14
21:00 - 22:00	0.00	0.00	336.37	40.34
22:00 - 23:00	0.00	0.00	266.08	37.94
23:00 - 00:00	0.00	0.00	265.85	38.83

Table 9 presents the electrical measurements for the LHI 1's performance. It is noted that at around 17:00, the TR sets reading went to zero, which indicates that the field had tripped at this stage.

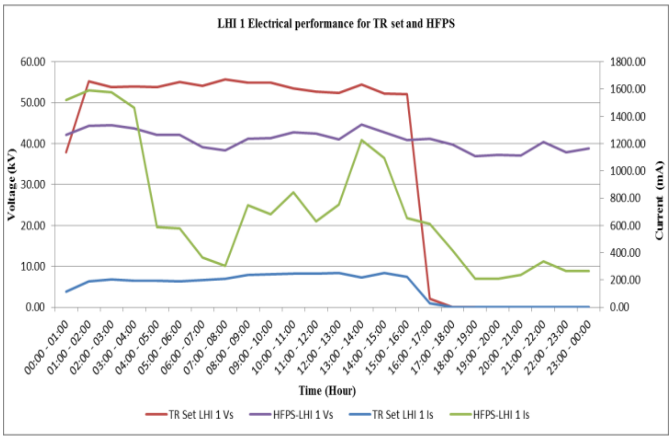

Figure 10: LHI 1 electrical performance for TR set and HFPS.

The installation on the HFPS on the LHI 1 did not result in an improved electrical performance although the current was not stable. Due to excessive sparking, probably caused by a loose discharge electrode wire.

Table 10: LHI 2 current and voltage measurement during the ESP efficiency tests for TR set and the new HFPS.

	LHI 2			
	TR Set LHI 2 Is	TR Set LHI 2 Vs	HFPS-LHI 2 Is	HFPS-LHI 2 Vs
00:00 - 01:00	206.10	20.73	1469.27	47.32
01:00 - 02:00	277.35	29.12	1614.40	49.24
02:00 - 03:00	274.12	30.28	1647.32	49.64
03:00 - 04:00	249.15	31.48	1653.02	50.26
04:00 - 05:00	241.07	30.52	1342.00	50.08
05:00 - 06:00	267.00	30.30	1336.98	50.08
06:00 - 07:00	256.93	30.52	823.38	47.95
07:00 - 08:00	263.83	30.12	450.97	45.50
08:00 - 09:00	281.15	31.57	1028.68	49.54
09:00 - 10:00	262.20	31.55	1213.70	50.49
10:00 - 11:00	278.52	31.48	1232.10	49.57
11:00 - 12:00	244.22	30.67	1171.17	49.05
12:00 - 13:00	224.48	30.07	1152.22	49.00
13:00 - 14:00	204.33	30.40	1480.20	49.68
14:00 - 15:00	185.38	31.07	1494.90	49.36
15:00 - 16:00	217.15	31.25	1098.67	47.88
16:00 - 17:00	170.02	29.45	923.10	48.13
17:00 - 18:00	217.63	29.58	678.33	47.40
18:00 - 19:00	248.85	30.82	245.02	42.51
19:00 - 20:00	269.32	30.82	257.27	42.83
20:00 - 21:00	286.85	30.28	278.17	43.10
21:00 - 22:00	290.20	31.00	447.43	46.62
22:00 - 23:00	299.03	29.80	353.35	45.36
23:00 - 00:00	283.87	30.05	325.88	45.17

Table 10 presents the electrical measurements for the LHI 2's performance. LHI 2's electrical performance is presented on figure 11, plotted from data acquired from table 10.

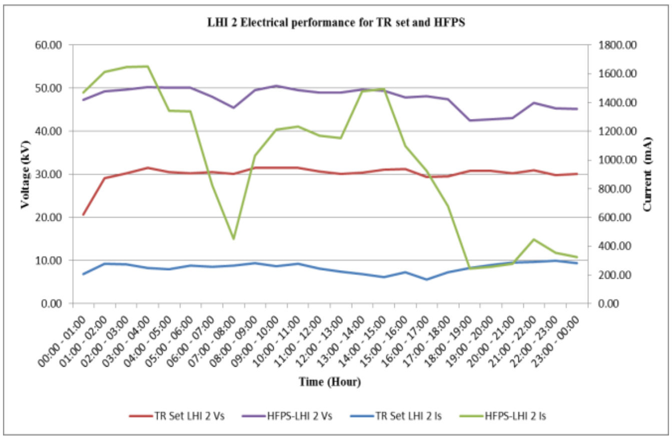

Figure 11: LHI 2 electrical performance for TR set and HFPS.

The LHI 2's performance was similar to that observed on LHI 1. The field was sparking excessively, thus not allowing stable operating conditions. The TR set was able to maintain consistent current as the controller allows for manual intervention and can be set to a point where it can operate without frequent trips due to sparking and arcing.

Table 11: LHI 3 current and voltage measurement during the ESP efficiency tests for TR set and the new HFPS.

	LHI 3			
	TR Set LHI 3 Is	TR Set LHI 3 Vs	HFPS-LHI 3 Is	HFPS-LHI 3 Vs
00:00 - 01:00	133.12	25.35	976.08	45.22
01:00 - 02:00	106.03	37.77	1461.02	48.82
02:00 - 03:00	83.43	38.38	1588.62	49.36
03:00 - 04:00	74.73	39.43	1661.70	49.54
04:00 - 05:00	86.23	38.90	1518.82	47.78
05:00 - 06:00	78.15	39.22	1544.50	48.47
06:00 - 07:00	89.07	39.32	1085.60	46.08
07:00 - 08:00	78.13	38.27	512.97	42.56
08:00 - 09:00	81.65	38.72	922.45	46.19
09:00 - 10:00	99.50	39.18	1188.33	47.22
10:00 - 11:00	94.35	39.63	1239.40	46.81
11:00 - 12:00	103.73	40.03	1141.73	45.93
12:00 - 13:00	70.37	38.20	1154.38	46.75
13:00 - 14:00	70.05	39.30	1390.77	47.66
14:00 - 15:00	50.67	37.47	1554.23	48.67
15:00 - 16:00	51.03	38.20	1230.05	46.50
16:00 - 17:00	31.93	37.22	930.72	44.72
17:00 - 18:00	29.93	37.50	737.08	43.95
18:00 - 19:00	37.75	38.02	200.40	39.56
19:00 - 20:00	42.03	38.97	168.37	39.17
20:00 - 21:00	47.20	38.45	161.68	39.05
21:00 - 22:00	47.45	39.38	300.50	43.28
22:00 - 23:00	51.22	39.42	208.97	42.27
23:00 - 00:00	53.21	38.97	200.72	41.77

Table 11 presents the electrical measurements for the LHI 3's performance.

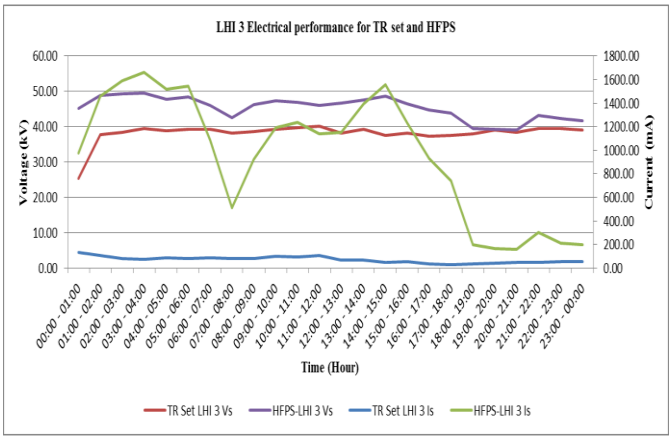

Figure 12: LHI 3 electrical performance for TR set and HFPS.

Figure 12 presents the electrical performance of the LHI 3's field. Similar to that of LHI 1 and 2, this field was also experiencing a high spark rate. The HFPS was still able to maintain a higher electrical performance than that of the TR set, in these upset conditions.

Table 12: LHI 4 current and voltage measurement during the ESP efficiency tests for TR set and the new HFPS.

	LHI 4			
	TR Set LHI 4 Is	TR Set LHI 4 Vs	HFPS-LHI 4 Is	HFPS-LHI 4 Vs
00:00 - 01:00	312.80	47.90	863.23	43.64
01:00 - 02:00	265.97	46.50	1356.82	47.99
02:00 - 03:00	373.50	47.07	1547.48	48.09
03:00 - 04:00	387.47	46.93	1647.63	48.36
04:00 - 05:00	350.93	47.20	1655.32	48.23
05:00 - 06:00	367.82	47.33	1655.33	48.23
06:00 - 07:00	360.53	47.28	1489.15	47.19
07:00 - 08:00	350.32	46.68	1042.40	45.72
08:00 - 09:00	379.12	47.28	1198.05	46.05
09:00 - 10:00	376.98	47.43	1517.92	47.70
10:00 - 11:00	356.15	46.53	1565.90	47.39
11:00 - 12:00	314.50	46.20	1607.87	48.24
12:00 - 13:00	254.43	44.55	1605.03	48.22
13:00 - 14:00	262.65	45.88	1636.20	47.54
14:00 - 15:00	244.80	46.57	1664.87	47.65
15:00 - 16:00	249.93	46.78	1541.83	46.70
16:00 - 17:00	144.67	47.77	1396.33	46.43
17:00 - 18:00	138.23	47.75	1226.12	45.40
18:00 - 19:00	174.97	47.17	521.98	43.16
19:00 - 20:00	189.20	47.33	312.25	41.03
20:00 - 21:00	191.10	48.00	279.85	42.21
21:00 - 22:00	179.20	46.85	419.53	43.03
22:00 - 23:00	200.68	48.33	387.60	42.74
23:00 - 00:00	176.00	47.51	365.08	43.23

Table 11 presents the electrical measurements for the LHI 3's performance. It is noted the performance decreased after 17:00. Figure 13 presents the performance of the LHI 4 as illustrated by the value of table 12.

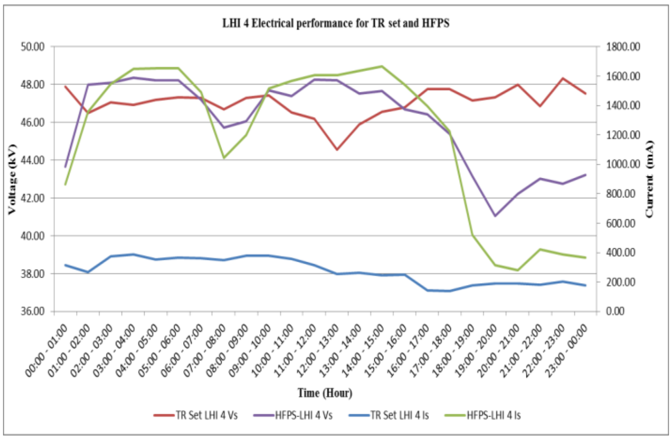

Figure 13: LHI 4 electrical performance for TR set and HFPS.

Similarly to all the other fields discussed, the installation of the HFPS resulted in improved electrical performance. Although this casing was experiencing excessive sparking, the HFPSs were able to maintain a high electrical performance than that which was possible with the TR sets.

Table 13: RHI 1 current and voltage measurement during the ESP efficiency tests for TR set and the new HFPS.

	RHI 1			
	TR Set RHI 1 Is	TR Set RHI 1 Vs	HFPS-RHI 1 Is	HFPS-RHI 1 Vs
00:00 - 01:00	426.52	34.97	1551.43	43.32
01:00 - 02:00	330.12	48.53	1647.20	46.50
02:00 - 03:00	370.23	50.82	1670.73	47.11
03:00 - 04:00	381.17	51.68	1631.80	46.11
04:00 - 05:00	343.73	51.68	1620.67	47.60
05:00 - 06:00	340.85	51.45	1618.08	47.63
06:00 - 07:00	324.25	51.57	1348.98	46.24
07:00 - 08:00	315.50	51.98	1080.42	45.44
08:00 - 09:00	325.93	51.78	1527.73	48.04
09:00 - 10:00	315.38	51.32	1327.35	45.94
10:00 - 11:00	311.13	50.90	1225.52	45.77
11:00 - 12:00	280.07	50.95	1521.20	47.85
12:00 - 13:00	306.80	52.47	1548.15	48.20
13:00 - 14:00	287.72	50.93	1582.92	45.33
14:00 - 15:00	265.85	50.65	1617.57	46.59
15:00 - 16:00	276.00	51.18	1634.65	46.66
16:00 - 17:00	293.62	50.32	1606.02	46.95
17:00 - 18:00	308.37	49.55	1416.68	46.66
18:00 - 19:00	313.90	49.97	828.20	43.46
19:00 - 20:00	289.07	49.98	931.95	42.96
20:00 - 21:00	311.80	48.27	960.98	44.18
21:00 - 22:00	335.70	51.22	913.72	44.06
22:00 - 23:00	329.68	49.70	1085.30	43.70
23:00 - 00:00	320.10	51.16	1120.83	44.56

Table 13, represents the electrical data for the RHI 1's performance.

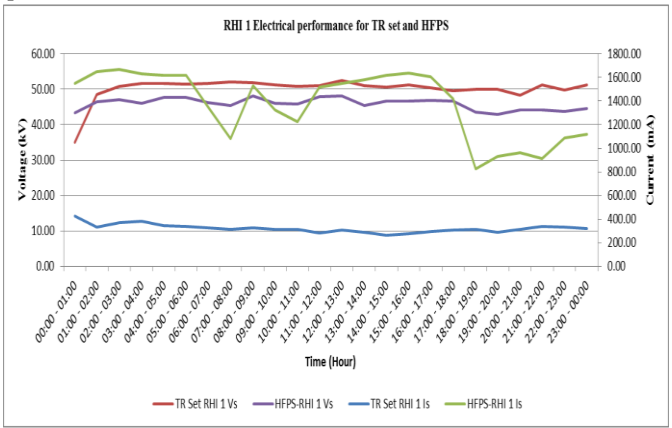

Figure 14: RHI 1 electrical performance for TR set and HFPS.

The RHI 1's electrical performance is plotted on figure 14. The TR set's performance for this field is typical of how low the electrical performance of the TR set can be more especially for the first field. The current input into the field was consistently below 350 mA with the TR set in operation. The installation of the HFPS saw the current input into the field increase to above 1000 mA. The voltage of the TR set was slightly above that which the HFPS could manage, however due to the inability to produce a high enough current; the high voltage has not significant influence on the collection of dust burden.

Table 14: RHI 2 current and voltage measurement during the ESP efficiency tests for TR set and the new HFPS.

	RHI 2			
	TR Set RHI 2 Is	TR Set RHI 2 Vs	HFPS-RHI 2 Is	HFPS-RHI 2 Vs
00:00 - 01:00	188.07	56.45	1567.45	43.40
01:00 - 02:00	272.15	56.37	1638.30	43.84
02:00 - 03:00	244.50	56.63	1671.55	44.81
03:00 - 04:00	207.82	56.67	1652.80	44.13
04:00 - 05:00	180.38	56.37	1605.73	43.52
05:00 - 06:00	164.28	55.60	1634.05	44.22
06:00 - 07:00	185.85	56.57	1631.70	45.80
07:00 - 08:00	212.20	57.03	1574.23	46.10
08:00 - 09:00	185.28	57.17	1620.02	46.09
09:00 - 10:00	174.87	56.85	1618.40	46.79
10:00 - 11:00	157.25	56.00	1601.98	46.28
11:00 - 12:00	143.80	56.22	1644.55	46.96
12:00 - 13:00	175.48	56.58	1644.10	46.79
13:00 - 14:00	145.05	56.02	1647.48	46.70
14:00 - 15:00	167.63	56.72	1629.02	45.23
15:00 - 16:00	182.40	57.02	1652.58	45.88
16:00 - 17:00	187.70	56.40	1627.35	45.85
17:00 - 18:00	172.12	56.28	1601.47	46.44
18:00 - 19:00	168.17	55.20	1524.87	47.06
19:00 - 20:00	159.57	55.50	1497.87	46.79
20:00 - 21:00	158.90	55.53	1564.35	47.33
21:00 - 22:00	202.30	56.90	1522.85	47.51
22:00 - 23:00	294.77	56.35	1584.85	47.65
23:00 - 00:00	347.46	58.33	1562.45	46.54

Electrical performance of the RHI 2 field is shown on table 14.

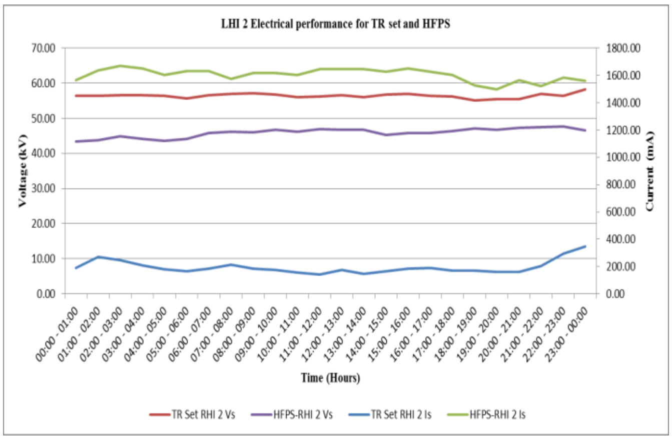

Figure 15: RHI 2 electrical performance for TR set and HFPS.

Figure 15, presented the graphical representation of the data on table 14. It is noted that the electrical performance of the HFPS surpassed that of the TR set, with the HFPS being able to input full load current into the field. The TR sets voltage is significantly higher than that of the of the HFPS, reason being the controller algorithm is such that was force the TR set to push the voltage as high as possible in order to achieved the desired 1600 mA. Since the HFPS is able to achieve full load operational current, at a lower voltage, it simple maintains the voltage level at which the full load current was achieved.

Table 15: RHI 3 current and voltage measurement during the ESP efficiency tests for TR set and the new HFPS.

	RHI 3			
	TR Set RHI 3 Is	**TR Set RHI 3 Vs**	**HFPS-RHI 3 Is**	**HFPS-RHI 3 Vs**
00:00 - 01:00	497.53	30.28	1652.45	43.98
01:00 - 02:00	616.63	42.27	1699.62	43.90
02:00 - 03:00	601.13	39.93	1643.02	42.36
03:00 - 04:00	572.45	40.05	1642.93	42.12
04:00 - 05:00	600.87	40.62	1642.88	42.38
05:00 - 06:00	629.07	40.90	1642.88	42.37
06:00 - 07:00	651.32	41.32	1696.70	43.90
07:00 - 08:00	724.08	42.33	1642.95	42.91
08:00 - 09:00	582.30	39.87	1671.18	43.88
09:00 - 10:00	577.13	39.88	1657.50	44.04
10:00 - 11:00	602.97	40.10	1669.70	44.30
11:00 - 12:00	619.62	41.58	1690.92	44.81
12:00 - 13:00	680.00	42.17	1642.98	43.81
13:00 - 14:00	610.43	41.72	1659.72	44.20
14:00 - 15:00	690.20	42.88	1671.17	43.94
15:00 - 16:00	698.00	43.55	1699.42	44.67
16:00 - 17:00	697.10	43.02	1642.78	43.33
17:00 - 18:00	718.33	43.82	1670.87	44.33
18:00 - 19:00	657.18	43.35	1642.35	44.12
19:00 - 20:00	651.42	42.68	1670.20	44.70
20:00 - 21:00	677.65	43.17	1642.73	44.04
21:00 - 22:00	707.18	43.98	1671.17	44.83
22:00 - 23:00	672.95	42.72	1639.28	44.29
23:00 - 00:00	704.13	43.05	1668.98	45.08

Table 15, illustrates the electrical performance data of the RHI 3 field.

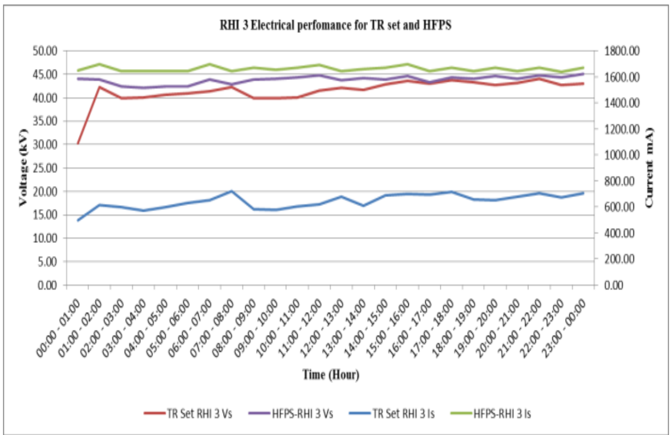

Figure 16: RHI 3 electrical performance for TR set and HFPS.

RHI 3's electrical performance is plotted on figure 16, it is noted that with the TR set in operation, the input current was significantly low. The installation of the HFPS resulted in maximum input current being fed into the field and maintained.

Table 16: RHI 4 current and voltage measurement during the ESP efficiency tests for TR set and the new HFPS.

	RHI 4			
	TR Set RHI 4 Is	**TR Set RHI 4 Vs**	**HFPS-RHI 4 Is**	**HFPS-RHI 4 Vs**
00:00 - 01:00	1309.22	39.12	1646.52	41.85
01:00 - 02:00	1618.05	47.18	1405.00	39.55
02:00 - 03:00	392.73	32.90	1636.85	41.71
03:00 - 04:00	1429.43	45.58	1635.08	41.12
04:00 - 05:00	1604.32	47.98	1668.53	41.34
05:00 - 06:00	1552.65	47.67	1668.55	41.35
06:00 - 07:00	1619.13	48.85	1365.77	39.34
07:00 - 08:00	1691.33	49.30	1620.80	41.52
08:00 - 09:00	1174.08	43.02	1671.65	42.68
09:00 - 10:00	615.10	36.02	1351.88	39.59
10:00 - 11:00	1657.02	49.33	1635.70	42.25
11:00 - 12:00	1579.98	47.88	1357.00	39.69
12:00 - 13:00	1635.52	49.20	1629.92	42.23
13:00 - 14:00	1649.02	49.50	1679.05	42.86
14:00 - 15:00	1590.63	48.82	1643.93	41.86
15:00 - 16:00	353.52	34.85	1323.10	39.25
16:00 - 17:00	1396.00	46.75	1674.47	42.83
17:00 - 18:00	1510.62	47.52	1640.17	42.13
18:00 - 19:00	1574.63	49.22	1506.48	40.75
19:00 - 20:00	1533.65	48.87	1430.17	40.11
20:00 - 21:00	1464.58	47.87	1697.60	43.18
21:00 - 22:00	1186.13	45.73	1614.52	41.71
22:00 - 23:00	747.35	41.38	1339.58	39.82
23:00 - 00:00	1559.51	48.85	1638.25	42.34

Table 16, illustrates the electrical performance data of the RHI 4 field. The RHI 4's electrical performance was not stable for both power supply technologies, as seen on figure 17.

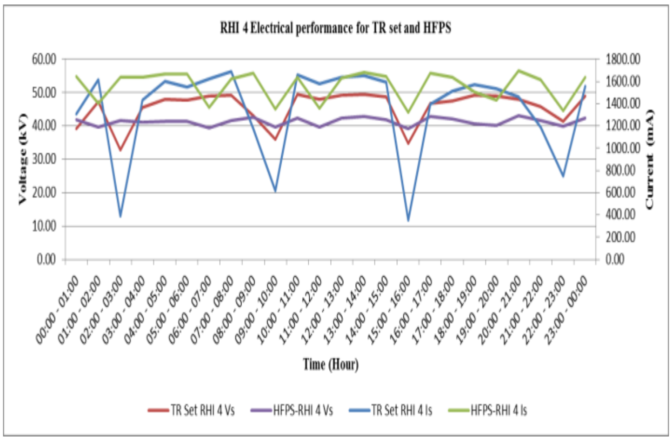

Figure 17: RHI 4 electrical performance for TR set and HFPS.

The performance of the field was within specification for both power supply technologies, although the field was experiencing excessive sparking resulting frequent performance dips.

Table 17: RHO 1 current and voltage measurement during the ESP efficiency tests for TR set and the new HFPS.

	RHO 1			
	TR Set RHO 1 Is	TR Set RHO 1 Vs	HFPS-RHO 1 Is	HFPS-RHO 1 Vs
00:00 - 01:00	485.65	24.03	26.88	9.85
01:00 - 02:00	585.53	24.93	15.97	10.51
02:00 - 03:00	561.22	24.80	19.22	11.36
03:00 - 04:00	617.95	24.28	14.03	11.14
04:00 - 05:00	635.83	24.63	15.38	10.90
05:00 - 06:00	603.37	24.30	15.38	10.87
06:00 - 07:00	623.03	23.95	15.32	11.16
07:00 - 08:00	668.65	24.80	21.37	12.29
08:00 - 09:00	659.20	24.07	19.05	11.63
09:00 - 10:00	651.07	23.93	16.97	11.11
10:00 - 11:00	735.33	25.10	19.03	11.26
11:00 - 12:00	673.78	25.33	17.72	11.05
12:00 - 13:00	840.45	25.72	18.95	11.57
13:00 - 14:00	677.05	24.87	22.20	11.45
14:00 - 15:00	925.17	23.40	18.87	11.38
15:00 - 16:00	1404.03	25.57	19.47	11.46
16:00 - 17:00	1323.68	26.62	16.88	11.21
17:00 - 18:00	1179.75	27.17	16.08	11.40
18:00 - 19:00	1155.28	27.00	18.10	11.44
19:00 - 20:00	1224.40	27.75	18.20	11.33
20:00 - 21:00	1245.72	28.53	16.72	11.36
21:00 - 22:00	1181.37	28.37	14.02	9.96
22:00 - 23:00	1217.65	28.25	18.73	12.53
23:00 - 00:00	1193.89	27.97	14.00	10.51

Table 17, illustrates the electrical performance data of the RHO 1 field. It was noted that by the time the HFPS was installed, that field had an internal fault, which was subsequently repaired during an opportunity.

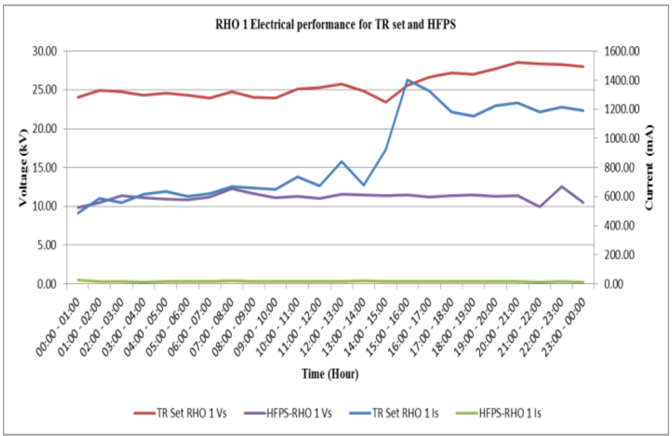

Figure 18: RHO 1 electrical performance for TR set and HFPS.

Figure 18 illustrates the performance of the RHO 1 field, unfortunately the field experienced an internal fault when the HFPS was installed and thus its performance could not be determined at the stage when the testing was conducted.

Table 18: RHO 2 current and voltage measurement during the ESP efficiency tests for TR set and the new HFPS.

	RHO 2			
	TR Set RHO 2 Is	TR Set RHO 2 Vs	HFPS-RHO 2 Is	HFPS-RHO 2 Vs
00:00 - 01:00	287.13	34.80	1529.67	45.75
01:00 - 02:00	788.55	56.03	1634.95	48.59
02:00 - 03:00	807.60	56.85	1642.23	48.82
03:00 - 04:00	754.15	57.22	1626.78	49.05
04:00 - 05:00	740.37	57.27	1568.45	48.90
05:00 - 06:00	741.88	57.40	1565.50	48.87
06:00 - 07:00	707.23	55.72	1311.33	46.83
07:00 - 08:00	727.90	57.23	990.22	44.15
08:00 - 09:00	718.97	57.57	1044.18	44.13
09:00 - 10:00	692.75	57.25	1109.02	46.23
10:00 - 11:00	663.82	55.58	1311.63	46.04
11:00 - 12:00	652.43	55.53	1162.78	44.94
12:00 - 13:00	644.18	56.23	1100.32	44.99
13:00 - 14:00	584.63	53.77	1319.40	45.85
14:00 - 15:00	655.05	55.77	1378.70	45.82
15:00 - 16:00	664.02	56.03	1506.88	47.43
16:00 - 17:00	715.52	56.52	1557.13	47.36
17:00 - 18:00	720.35	56.38	1433.12	47.34
18:00 - 19:00	765.55	57.27	1200.15	45.88
19:00 - 20:00	746.07	57.00	1173.95	45.94
20:00 - 21:00	738.70	57.07	1106.00	44.97
21:00 - 22:00	745.47	56.57	1044.87	44.91
22:00 - 23:00	784.58	57.30	1150.53	46.27
23:00 - 00:00	740.03	56.41	1219.43	46.82

Table 18, illustrates the electrical performance data of the RHO 2 field. The performance of this field was within specification for both power supply technologies. The TR set was able to produce and maintain a current input of above 700 mA at a voltage level of 57 kV, exceptional performance for a TR set more especially that it is operating on the second field. The installation of the HFPS further improved the electrical performance of the field, with current exceeding a 1000 mA. Figure 19 presents the plotted data as shown on table 18.

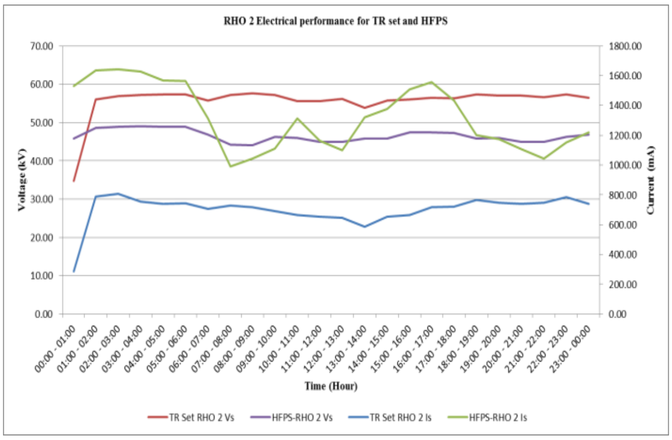

Figure 19: RHO 2 electrical performance for TR set and HFPS.

Table 19: RHO 3 current and voltage measurement during the ESP efficiency tests for TR set and the new HFPS.

	RHO 3			
	TR Set RHO 3 Is	TR Set RHO 3 Vs	HFPS-RHO 3 Is	HFPS-RHO 3 Vs
00:00 - 01:00	424.88	20.72	1528.97	40.16
01:00 - 02:00	279.42	32.67	1660.88	42.58
02:00 - 03:00	221.15	32.08	1699.50	43.16
03:00 - 04:00	228.88	32.85	1642.48	41.61
04:00 - 05:00	227.42	32.98	1645.20	42.07
05:00 - 06:00	208.53	32.55	1645.22	42.08
06:00 - 07:00	204.32	32.83	1698.63	43.52
07:00 - 08:00	186.42	33.62	1641.25	43.14
08:00 - 09:00	179.73	32.93	1661.88	43.47
09:00 - 10:00	180.73	32.98	1636.35	42.92
10:00 - 11:00	165.62	33.08	1663.05	43.56
11:00 - 12:00	158.77	32.40	1661.12	43.65
12:00 - 13:00	155.83	32.08	1649.32	43.33
13:00 - 14:00	143.00	32.13	1648.33	43.04
14:00 - 15:00	169.88	34.93	1665.90	42.98
15:00 - 16:00	258.68	38.85	1649.60	42.77
16:00 - 17:00	292.80	38.30	1646.85	42.91
17:00 - 18:00	380.17	39.68	1669.48	43.15
18:00 - 19:00	396.23	39.58	1631.75	42.64
19:00 - 20:00	386.58	39.43	1641.15	42.43
20:00 - 21:00	379.28	38.90	1670.38	43.69
21:00 - 22:00	402.30	40.07	1683.55	44.05
22:00 - 23:00	379.90	40.53	1639.33	43.29
23:00 - 00:00	423.15	40.08	1695.53	43.97

Table 19, illustrates the electrical performance data of the RHO 3 field. The TR set showed poor performance with, with a current input into the field being below 200 mA, such poor performance is typical due to internal fault condition such as a defective rapping system. A shearing pin was replaced on the discharge electrode rapping system and with the installation on the HFPS, the input current into the field went to maximum. Figure 20 shows the contrasting performances of the two power supply systems.

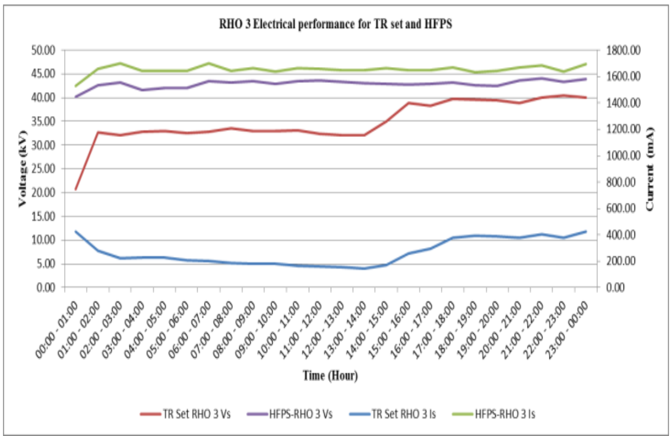

Figure 20: RHO 3 electrical performance for TR set and HFPS.

Table 20: RHO 4 current and voltage measurement during the ESP efficiency tests for TR set and the new HFPS.

	RHO 4			
	TR Set RHO 4 Is	TR Set RHO 4 Vs	HFPS-RHO 4 Is	HFPS-RHO 4 Vs
00:00 - 01:00	768.27	21.97	1584.35	40.34
01:00 - 02:00	1642.20	34.53	1642.85	42.02
02:00 - 03:00	1652.28	34.68	1699.47	43.19
03:00 - 04:00	1665.53	34.87	1671.13	42.33
04:00 - 05:00	1707.78	35.18	1667.25	41.90
05:00 - 06:00	1665.07	34.98	1667.27	41.89
06:00 - 07:00	1675.15	35.78	1699.48	42.77
07:00 - 08:00	1632.97	35.47	1642.85	41.69
08:00 - 09:00	1690.55	35.92	1675.27	42.72
09:00 - 10:00	1666.40	35.75	1674.75	42.90
10:00 - 11:00	1669.43	35.70	1661.23	42.99
11:00 - 12:00	1698.65	35.23	1670.68	42.77
12:00 - 13:00	1619.53	34.85	1688.67	43.32
13:00 - 14:00	1443.42	33.98	1669.82	43.16
14:00 - 15:00	1600.03	35.23	1641.90	42.59
15:00 - 16:00	1669.95	35.72	1670.23	42.91
16:00 - 17:00	1602.93	35.48	1681.37	43.77
17:00 - 18:00	1607.60	35.83	1698.48	43.93
18:00 - 19:00	1694.03	36.28	1677.83	43.81
19:00 - 20:00	1678.10	36.25	1685.17	43.57
20:00 - 21:00	1590.17	36.08	1670.42	43.07
21:00 - 22:00	1655.37	36.15	1670.90	42.89
22:00 - 23:00	1628.87	36.25	1642.50	42.49
23:00 - 00:00	1635.57	36.31	1671.03	43.08

Table 20, illustrates the electrical performance data of the RHO 4 field. The RHO 4's performance was within specification with the TR set installed, as it was able to produce maximum current. The installation of a HFPS result in the HFPS maintaining the maximum current as well, however it managed to increase the input voltage into the field as well. Figure 21, presents the graphical plot of the data presented on table 20, for the performance of the RHO 4 field.

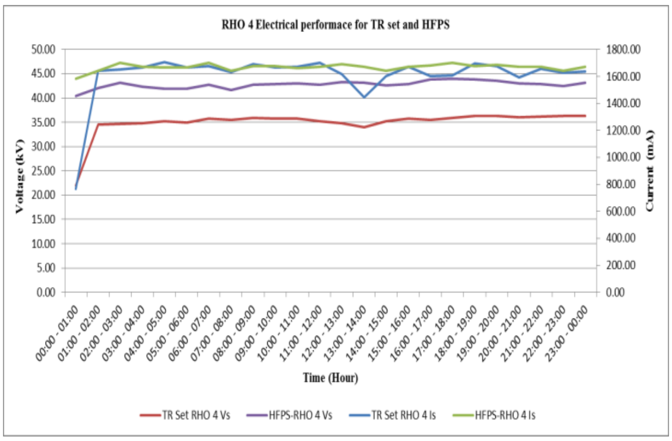

Figure 21: RHO 4 electrical performance for TR set and HFPS.

The overall electrical performance of the two power supply technologies has shown that the new HFPS have a, better electrical conversion efficiency as compared to that of the TR set. The LHO casing had a maximum power input of 228 kW, with TR set in operation, whereas the new HFPS was able to produce a maximum power input of 389 kW. This gave a casing power input increase of 41%. The LHI casing had a maximum power input of 237 kW, with TR set in operation, whereas the new HFPS was able to produce a maximum power input of 419 kW. This gave a casing power input increase of 43%.

The RHI casing had a maximum power input of 253 kW, with TR set in operation, whereas the new HFPS was able to produce a maximum power input of 403 kW. This gave a casing power input increase of 37%. The highest power input into the RHO casing was 275 kW for conventional TR sets, whereas the highest for a casing with new HFPS installed went up to 420 kW.

This gave a casing power input increase of 35%. The overall electrical performance increase of the ESP casings is, expected to result in improved collection efficiency of the ESP.

Emissions performance comparison

Figure 22 illustrates the emissions performance of the unit, it can, be, seen how the emissions reduced and consistently maintained at low levels.

The emissions recorded shows that for the period in which the conventional TR sets were in operation the emissions were low; however the inconsistency in the electrical performance of the TR sets, resulted in a fluctuation of the emissions. At the time, when all 16 new HFPS were installed and fully operation, it could be seen that the emissions reduced and were maintained, this is due to the consistency that the new HFPS are able to maintain high electrical power input into the ESP.

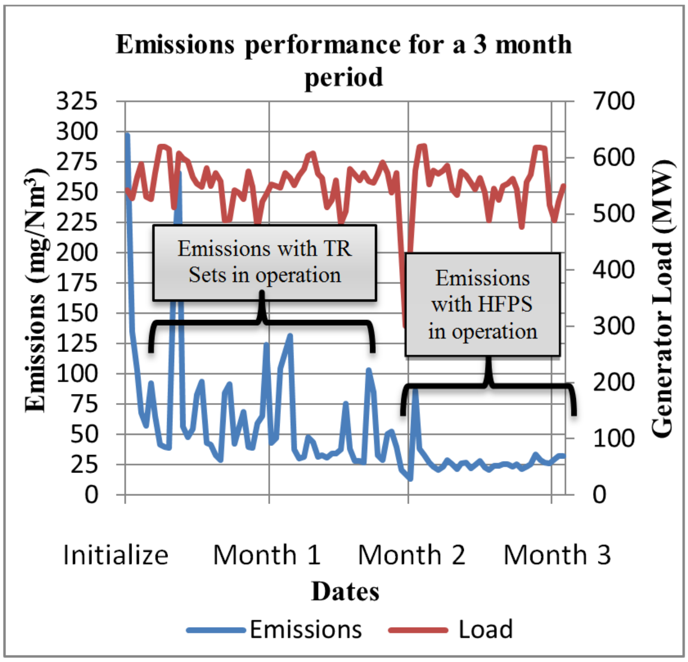

Figure 22: Emissions performance.

The ESP efficiency test showed that the ESP was emitting 42.8 mg/Nm^3 with conventional TR sets installed, and 19.3 mg/Nm^3 with new HFPS transformers installed in the front four fields of all the casings. The reduction in emission was 45%, which is extremely significant. Particulate emissions are, governed by the air quality legislation, which requires the operation of a power station to comply with the stipulated emissions limits at all times during operation.

Failure to comply with stipulated emissions limits as specified by the legislation carries a stiff fine or even jail time. In order to comply with the set out emissions limits, power stations have resorted to taking load losses; reduction in boiler production capacity in order to reduce particulate emissions. The practice of taking load losses due to ineffective ESP performance is a costly exercise, as the power station loses revenue for every MW that is not generated. This chapter will discuss the exact cost implications of operating with ineffective ESPs that result in units having to take load losses in order to meet emissions limits.

Cost of emissions

A power station that is, rated for 618 MW, full load production is required to maintain emissions below 100 mg/Nm^3, daily. Thus, if a unit is unable to maintain emissions below 100 mg/Nm^3, a 118 MW load loss is typically taken during of peak periods. Off peak, periods are from 10:00 am to 17:00 pm and 22:00 pm to 05:00. This means a unit can run on average 10 hours a day with a 118 MW load loss, which is equivalent to 1.2 GWhrs of power that is, not generated during that period. That is 19% of the full load generating capacity that is lost, due to high particulate emissions.

The national electricity supplier has been struggling to meet the country's electricity demand since early 2007. A reduction in production is not ideal as it further puts pressure on the organisation and increases the likelihood of load shedding being, implemented in the country. The revenue loss because of these load losses is also significant, as it limits the suppliers' cash flow. Figure 23, illustrates bar graph representation of the generated load to the load loss taken as a result of high emissions.

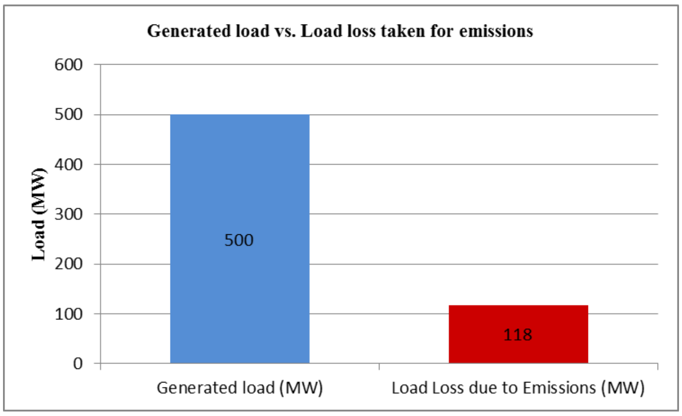

Figure 23: Graphical representation of the load loss and generated load in MW.

If a power station charges ZAR 88.66 per MWhr, running a 118 MW for 10 hours on average a day, that power station will incur a loss of ZAR 104,618.8 per day, which translates to

ZAR 2,929,326.40 per month. This is a significant loss of revenue; 19% of the possible ZAR 15,341,726.40 that a unit operating without high stack emissions load losses can generate. Figure 24 show the pie chart representation of this revenue loss, surfed as a result of emissions.

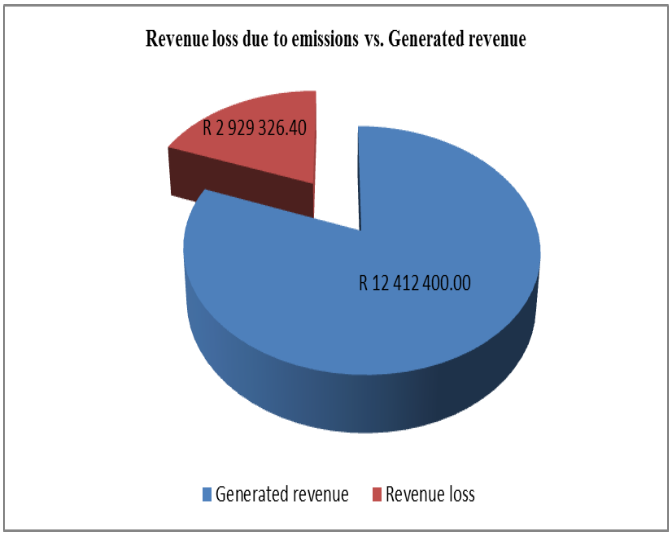

Figure 24: Graphical representation of the revenue loss and generated revenue.

During the summer periods, emissions levels become relatively high due to the high ambient temperatures that affect the process conditions; i.e. condenser back end pressures requiring the boiler to fire more in order to produce the required MWs. This, results in the ESP seeing a significant amount of flue gas volume flow result in ESP not being able to maintain low emissions. South African summer periods are from mid-October to mid-February, that a potential 5 months in which regular load losses can, be, taken to maintain emissions below legislations limits. Regular load losses for a period of 5 months could result in a revenue loss of approximately ZAR 16,000,000.

The return on investment for the project is realised within a two year period. The cost of the HFPS retrofit project was ZAR 25,000,000, per unit and based on the revenue loss due to the frequency and duration of load losses that power station takes in order to reduce particulate emissions. The, station would be able to obtain a return in investment on money spend to retrofitting existing ESPs with new HFPS, over a period of 2 years. As the new HFPS, technology is able to; consistently maintain emissions below the set emissions limits and thus, eliminating the need to maintain emissions with reduction of load.

CONCLUSION

The retrofit installation of the new HFPS transformer sets on to an existing ESP plant resulted in increased power input into the ESP fields. The observed power input increase into the fields, is as a result of the new HFSP ability to maintain high voltage and current inputs into the fields and its rapid response to sparking within the ESP. Deutch's, ESP collection efficiency suggest that the collection efficiency is directly influenced by the power available to the ESP. The new HFPS's ability to provide more power as compared to TR sets, resulted in a 45% reduction in particulate emissions.

The improved collection efficiency of the ESP will result in a financial benefit for the power station, as the likelihood of taking prolonged load losses due to high emissions has been addressed by the installation of the new HFPS transformer sets.

However, it was noted that, mechanical defects present in an ESP significantly hamper the performance of the field, regardless of the power supply technology implemented. Thus, it is of utmost importance to make sure that an ESP is kept in a mechanically sound condition.

REFERENCES

[1] H.J. White, "Industrial electrostatic precipitation," London, UK: Addison-Wesley, 1963.

[2] K.R. Parker, "Electrical operation of electrostatic precipitators", IEE Power and Energy Series, No. 41, London, The Institute of Engineering and Technology, 2003.

[3] TAPC, "Electrostatic precipitator", Total Air Pollution Control, pp. 1-8, 2018.

[4] S. Ostanek. Electrostatic precipitator operation, Neundorfer, pp. 1-22, 1998.

[5] E. Lami, F. Mattachini, R. Sala, H. Vigl, "A mathematical model of electrostatic field in wires-plate electrostatic precipitators", Journal of Electrostatics, Vol. 39, No. 1, pp. 1-21, 1997.

[6] R. Lytle, "Electrostatic precipitators", Hamon Research, pp. 1-4, 2018.

[7] G. Chauke and R. Gouws, "Fly ash resistivity profiling for South African coal fired power stations", Journal of Energy and Power Engineering, Vol. 12, No. 12, pp. 2306-2311, 2013.

[8] ISO 9096 - Stationary source emissions, Manual determination of mass concentration of particulate matter, International Organization for Standardization, No. 3, pp. 1-43, 2017.

[9] J.H. Turner, P.A. Lawless, T. Yamamoto, D.W. Coy, G.P. Greiner, J.D. McKenna, and W.M. Vata-vuk, Electrostatic precipitators. In A.J. Buonicore and W.T. Davis (Eds.), Air Pollution Engineering Manual Air and Waste Management Association. New York: Van No strand Reinhold, 1992, pp. 89-113.

[10] J.R. Mihelcic and J.B. Zimmerman, "Electrostatic precipitators". Section 12.8.4, Mines and Lackey, 2015.

[11] R. Guenther and H. Herder (2006), "High frequency switch mode power supplies for electrostatic precipitators operational and installation advantages", ICESP X, paper 7A1, pp. 1-10, 2006.

[12] Laurentiu-Marius Dumitran et al., "Particle charging in

combined corona-electrostatic fields", IEEE Transactions on Industry Applications, Vol. 44, No. 5, pp. 1429-1434, Sept.-Oct. 2008.

[13] H. Ziedan et al. "Onset voltage of corona discharge in wire-duct electrostatic precipitators" International Journal of Plasma Environmental Science and Technology, Vol. 4, No. 1, pp. 36-44, 2010.

[14] P.A. Lawless and L.E. sparks, "A mathematical model for calculating effects of back corona in wire-duct electrostatic precipitators". Journal of Electrostatics, Vol. 51, No. 1, pp. 242-256, 1980.

[15] S. Cristina, G. Denelli, and M. Feliziani. "Numerical computation of corona space charge and V-I characteristic in DC electrostatic precipitators", IEEE Transactions on Industry Applications, Vol. 27, No. 1, pp. 147-153, 1991.

[16] R. Standring, Method implementation document for EN 13284-1, BS EN 13284-1: 2002 - Stationary source emissions – Determination of low range mass concentration of dust – Part 1: Manual gravimetric method, Environment Agency, pp. 1-19, 2011.

[17] D.F. Johnston, M.M. Mahler, T.L. Farmer and R.E. Hummell, Apparatus and method for filtering voltage for an electrostatic precipitator, U. S. Patent 6839251, 2012.

[18] O. Dobzhanskyi and R. Gouws, "Study on energy savings applying highly efficient permanent magnet motor with two degrees of mechanical freedom in concrete industry", 10th International Conference on the Industrial and Commercial Use of Energy, pp. 101-105, 2013.

[19] R. Gouws, "Measurement and verification of load shifting interventions for a fridge plant system in South Africa", Journal of Energy in Southern Africa, Vol. 24, No. 1, pp. 9-14, 2013.